Data Repository Item 2011168

Methods

Nd was extracted from the hydrogenous and authigenic Fe-Mn oxyhydroxide fraction of marine sediment samples following the technique of Gutjahr et al. (2007) with slight modifications. An average of 70 mg of sediment per sample was decarbonated in 8 ml of 0.1 M Na acetate-buffered acetic acid for 24 hours, after which the supernatant was discarded and the sediments rinsed in deionised water (Milli-Q+ system) and centrifuged multiple times. Loosely adsorbed ions were removed by an exchangeable leach in 8 ml of 1 M $MgCl_2$ for ~1.5 hours, before further multiple rinsing in deionised water and centrifugation. The Fe-Mn oxyhydroxide fraction was solubilised in 8 ml of 50 mM hydroxylamine hydrochloride (HH) dissolved in 15% glacial acetic acid over a three hour period, during which the samples were gently agitated. The samples were further centrifuged before transfer of 6 ml of the supernatant to Teflon vials for drying.

Separation and purification of Sr and Nd from the matrix followed the procedure of Vance et al. (2004). The samples were processed through a 770 µl column of Biorad AG50W-X8 cation exchange resin, following which the Sr cut was converted to nitrate and processed through a 60 µl column of Eichrom Sr Spec resin. Nd purification was carried out using a 500 µl column containing Eichrom Ln resin.

Measurements of Sr and Nd isotopes were carried out on a Thermo-Finnigan Neptune MC-ICPMS at the Bristol Isotope Group (BIG) over a period of 18 months (Tables DR1 to DR3). The methodology for Nd isotope measurement is outlined in Vance and Thirlwall (2002). For both Sr and Nd, between 9 and 14 separate analyses of the NIST SRM 987 Sr standard or the La Jolla Nd standard were measured during each analytical session. The reproducibility of these 9 to 14 measurements (2 SD) was typically between 0.000007 and 0.000015 for $^{87}Sr/^{86}Sr$ and between 0.000005 and 0.000011 ($2\sigma \leq 0.21\ \varepsilon_{Nd}$) for $^{143}Nd/^{144}Nd$. Measured data on samples were re-normalised to take account of different average NIST SRM 987 $^{87}Sr/^{86}Sr$ or La Jolla $^{143}Nd/^{144}Nd$ between different analytical sessions (using normalising values of 0.710247 and 0.511856, respectively). The long-term reproducibility of the mass spectrometric analyses is best taken as two standard deviations of the 9 to 14 analyses of the standards conducted per analytical session. Previous assessments of the reproducibility of the leaching approach, in accessing exactly the same pool of Nd (Gutjahr et al. 2008), has shown that duplicate leaching experiments agree to 0.4 epsilon units (n = 10) on average, as compared to an instrumental reproducibility of 0.27 units for that study.

Age model

Site 980 core material is well characterised, with published $\delta^{18}O$ and $\delta^{13}C$ records (e.g. McManus et al., 1999). The age model used in this study is based on the orbitally tuned benthic $\delta^{18}O$ chronology of McManus et al. (1999) that was graphically correlated to existing deep sea chronologies published by Martinson et al. (1987) and Shackleton et al. (1990). The

age of samples in this study was determined by linear interpolation to the $\delta^{18}O$ chronology, which has a resolution of ~1.2 kyr.

Source of the Fe-Mn oxyhydroxide fraction

In view of the substantial deposition of terrigenous debris during the last glacial and deglaciation at Site 980, the possibility exists that the Nd extracted during the Fe-Mn oxyhydroxide leach may contain some contribution from the detrital fraction and/or input of "pre-formed" Fe-Mn oxyhydroxides (i.e. of terrigenous origin). We demonstrate below that this scenario is unlikely by comparing the Fe-Mn oxyhydroxide ε_{Nd} record to the detrital ε_{Nd} and Sr isotope records, as well as records of downcore ice-rafted debris (IRD) occurrence.

The detrital fraction has less radiogenic ε_{Nd} compositions than the Fe-Mn oxyhydroxide fraction, with ε_{Nd} ranging between -14.1 and -11.7 and an average offset between the Fe-Mn oxyhydroxide and detrital fractions of ~3.0 ε_{Nd} units (Tables DR1 and DR2). Based on the data compilation of Jeandel et al. (2007), corresponding sources of continental detrital material have Nd isotope compositions in the range of ~-14 to -12 in the circum-North Atlantic and GIN Seas regions (i.e. Scandinavia, most of the British Isles, Svalbard and a very small area of NE Greenland).

Analysis of the Sr isotope composition in the Fe-Mn oxyhydroxide fraction has been used by other workers to evaluate the integrity of the marine origin of the Fe-Mn oxyhydroxide fraction by comparison to the seawater $^{87}Sr/^{86}Sr$ composition (e.g. Rutberg et al., 2000). The Sr isotope compositions of leachate samples in this study (Figure DR1 and Table DR3) indicate a maximum difference from seawater of 0.0028 towards more radiogenic values. Given Sr/Nd ratios for detrital and Fe-Mn oxyhydroxide material (Gutjahr et al. 2007), and given the ε_{Nd} and $^{87}Sr/^{86}Sr$ ratios of the detritus (~-13 and ~0.725 respectively), such a deviation in $^{87}Sr/^{86}Sr$ would imply a maximum shift in the ε_{Nd} of the leachate due to contamination by the bulk detritus that is less than the analytical uncertainty (c.f. calculations in Gutjahr et al., 2007). Input of pre-formed Fe-Mn oxyhydroxides could cause a greater shift in the Nd isotopic composition of the leachate, assuming detrital $^{87}Sr/^{86}Sr$ in the pre-formed inputs, given that Sr/Nd ratios in pre-formed versus marine oxides are presumably sub-equal. Even in this case, however, the predicted maximum shift in ε_{Nd} is 0.5 epsilon units for the sample with the greatest Sr isotope shift. In addition the $^{87}Sr/^{86}Sr$ of pre-formed oxides are likely to be more radiogenic than the detrital fraction in view of preferential release of ^{87}Sr during glacial weathering (Hagedorn and Hasholt, 2004).

The leaching of volcanic debris is a more realistic possibility, given the proximity of Iceland to the core site, and is harder to rule out on the basis of the Nd and Sr isotope compositions in the Fe-Mn oxyhydroxide fraction alone. Typical ε_{Nd} compositions of Icelandic igneous rocks are ~+7 whereas Sr isotope compositions are ~0.7033 (Mertz and Haase, 1997). The amount of volcanic debris in the sediments is small enough that it does not greatly affect the overall Nd and Sr isotope composition of the *detrital* fraction, but the more reactive nature of volcanic debris means that it could have a non-negligible effect on the Sr and Nd isotope compositions of the Fe-Mn oxyhydroxide fraction should *in situ* leaching

occur within the sedimentary pile. However, none of the Fe-Mn leachates have a Sr isotope composition significantly below seawater, thus ruling out any contamination by volcanic debris on its own. It is *theoretically* possible that leaching of volcanic debris and other detritus together could co-incidentally maintain Sr isotopic compositions close to seawater and mask contamination of the Nd isotope signature.

In order to discount this possibility, we compare the ε_{Nd} Fe-Mn oxyhydroxide record to records of IRD occurrence from nearby core site MD01-2461 in the Porcupine Bight (Peck et al., 2007; Figure DR2). Some correlative change in both ε_{Nd} and IRD records is expected during Heinrich events in response to mass calving of icebergs and its effect on both thermohaline circulation and delivery of IRD. In Figure DR2, the systematic changes in ε_{Nd} are not mirrored in each of the IRD records. Panel (A) shows that British Ice Sheet (BIS) debris peaks during Heinrich event 2 with much reduced fluxes during the rest of the glaciation and deglaciation. In panel (B), the presence of tephra and volcanics shows peak occurrences during Heinrich events 1, 2 and 3, similar to the radiogenic shifts in ε_{Nd}, but crucially the greatest abundance of tephra occurs during the Younger Dryas when there is no appreciable change in the ε_{Nd} record. Furthermore, the peak in ε_{Nd} at ~20 kyr has no corresponding peak in the tephra and volcanics record. Finally, panel (C) presents the total IRD flux, and the shifts in the ε_{Nd} record appear independent of IRD abundance.

To conclude, the changes in the ε_{Nd} record are not considered to be due to either preformed inputs or to significant leaching of detrital material.

Mixing proportions of different water masses

On the basis of modern day, direct density observations of the water masses across the Wyville Thomson Ridge, Norwegian Sea Deep Water (NSDW) is estimated to constitute ~45% of Wyville Thomson Ridge Overflow Water (WTROW), with the remainder being made up of the overlying North Atlantic Current (NAC) (Sherwin et al., 2008; Sherwin and Turrell, 2005). Using these proportions and the ε_{Nd} compositions of NSDW of -7 and of the NAC of -13 (see the range of ε_{Nd} values at Station 23 in Figure 2 of the paper), the resulting calculated ε_{Nd} of WTROW is -10.3, which is very similar to the measured value for our record in the late Holocene of -10.2±0.3. Note that the Nd concentrations in the North Atlantic Current and WTROW water do not differ substantially. In the North Atlantic, the Nd concentration profile measured at Station 12 varies between ~2.5 and 2.9 x 10^{-12} g/g (Lacan and Jeandel, 2005). At Station 23 in the Faroe-Shetland Channel, the Nd concentration profile varies between ~2.4 and 3.5 x 10^{-12} g/g (Lacan and Jeandel, 2004).

Catastrophic drainage of Lake Agassiz

The outburst, dated at 8.47±0.3 kyr by ^{14}C measurements (Barber et al., 1999), may have occurred as two or more closely timed pulses (e.g. Clarke et al., 2004; Ellison et al., 2006; Hillaire-Marcel et al., 2007). The total estimated volume of water released varies between 1 and 2 x 10^{14} m^3 (Barber et al., 1999; Teller et al., 2002; Clarke et al., 2004) and up to 5 x 10^{14} m^3 (von Grafenstein et al., 1998). Rather than being confined to narrow bedrock

channels as with previous outbursts, this last outburst of Lake Agassiz passed through a breach in the decaying Laurentide Ice Sheet (LIS) and exited via the Hudson Strait, which is thought to have led to exceptionally rapid drainage and a potential freshwater flux of ~5 Sv if drainage occurred within 1 year or less (Clarke et al., 2004; Teller et al., 2002).

Lakes Agassiz and Ojibway were located on the Canadian Shield, the bedrock of which has ε_{Nd} between -44 and -15 (Goldstein and Jacobsen, 1987). Drainage of subglacial meltwater into the lakes carried Nd released by weathering of local glacial debris, and implies the ε_{Nd} of the lake water would be equally unradiogenic. The question remains whether the Lake water would carry enough Nd of sufficiently different isotope composition to impact the ε_{Nd} of the North Atlantic surface ocean, leading to the possibility of using ε_{Nd} records preserved in marine proxy archives to investigate the timing of the event as well as the mixing and propagation of the freshwater signal in the North Atlantic. The negative excursion in the ε_{Nd} record from Site 980 is potentially an indicator of this extraneous addition of unradiogenic Nd .

The short duration of the event (~1 year) implies that only the very highest resolution proxy records can detect the drainage event, and the record from Site 980 does not have that quality of resolution. However, the advantage of Nd is its ~1000 year residence time in the North Atlantic. The instantaneous addition of substantial quantities of unradiogenic Nd to the North Atlantic, combined with its long residence time, implies that the catastrophic drainage of Lake Agassiz would cause a sudden shift in North Atlantic surface and deep water ε_{Nd} that would linger for a considerable period of time.

Taking a volume of Lake water from the lower end of the proposed range of 2×10^{14} m^3 and an estimated concentration of Nd in the Lake water of 20 to 200 ppt, based on observations of the range in modern day river concentrations in North America (Goldstein and Jacobsen, 1987), the mass of additional Nd released into the Labrador Sea over the space of ~1 year is between 4 and 40 kilotons. The minimum effect of the drainage event on North Atlantic surface ocean ε_{Nd} can be estimated by calculating the potential change induced by distributing the total Nd released over the whole surface ocean of the North Atlantic and surrounding ocean basins. The values used to calculate the effect of the drainage event on North Atlantic surface ocean ε_{Nd} are listed in Table DR4. Note that the surface ε_{Nd} in the modern Labrador Sea is -20 (Lacan and Jeandel, 2005), so that a value of -25 ε_{Nd} of the drainage waters is considered reasonable. Using these values and a release of 2 kilotonnes of Nd, the North Atlantic would see a shift in ε_{Nd} from -14.0 to -15.2, whereas the Norwegian Sea would see a shift from -13.0 to -14.3 ε_{Nd}. The resultant mixing of NAC (shifted to -14.3) and NSDW (-7) in the same proportions as indicated above would result in WTROW of -11.

Given that surface ocean currents are thought to have constrained the initial spread of Lake Agassiz Nd, with a substantial proportion directed to the GIN Seas by the sub-polar gyre current (Born and Levermann, 2010), the observed shift to -12.3 at 7.9 kyr in the Feni Drift record could be feasibly generated by the drainage event. This scenario depends heavily on the total Nd released by the drainage event, which as yet remains unconstrained.

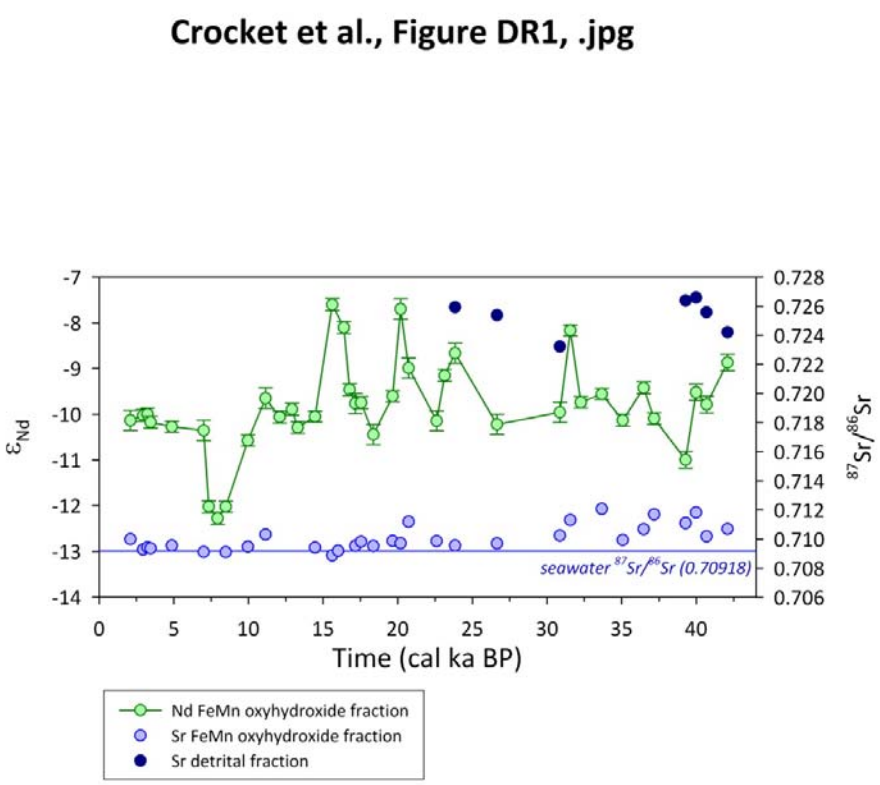

Figure DR1: The $^{87}Sr/^{86}Sr$ compositions of the Fe-Mn oxyhydroxide and detrital fractions with reference to the ε_{Nd} (ε; parts per 10^4 variation of $^{143}Nd/^{144}Nd$ ratio relative to $^{143}Nd/^{144}Nd_{CHUR}$ of 0.512638 (Jacobsen and Wasserburg, 1980)) trend in the Fe-Mn oxyhydroxide fraction.

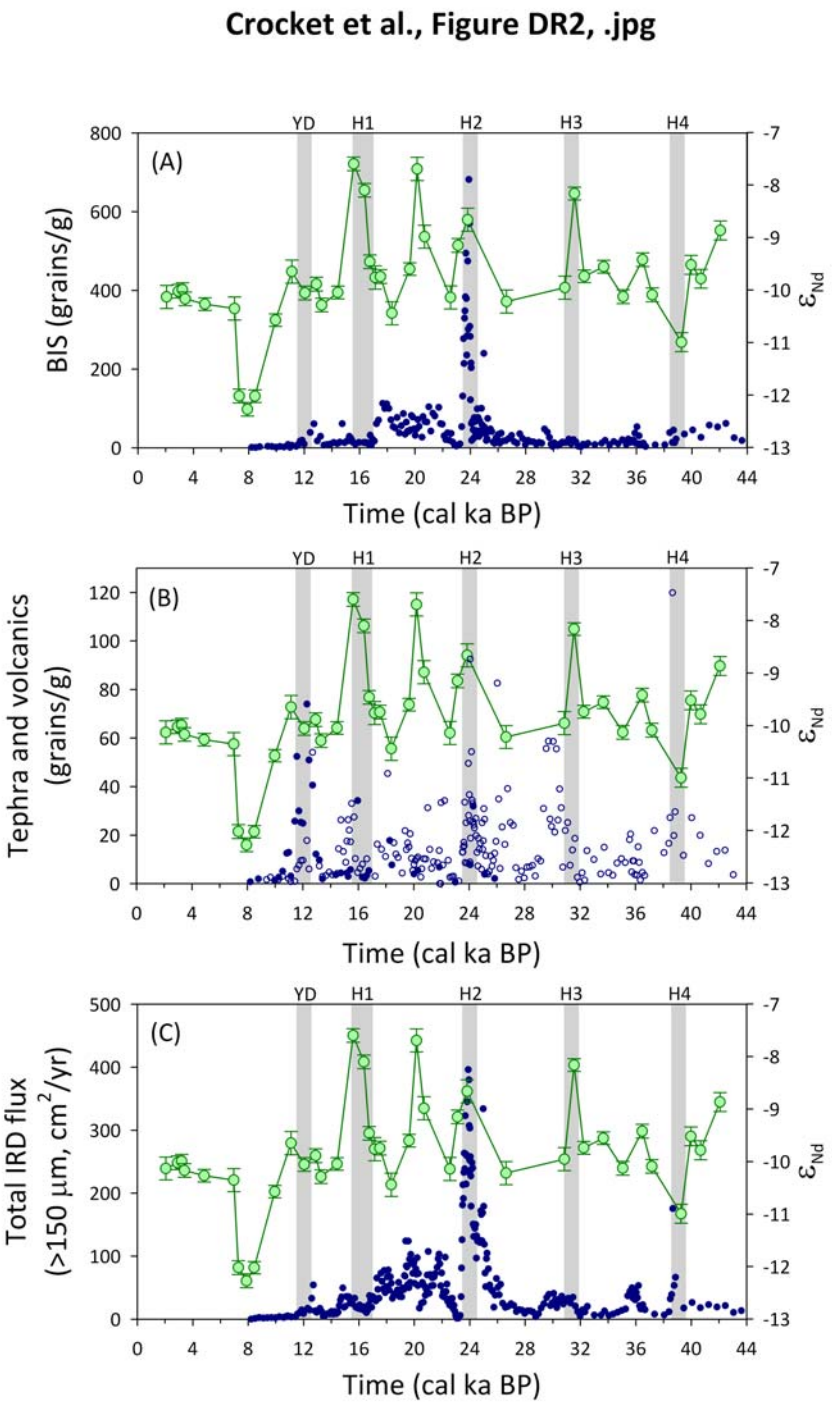

Figure DR2: Comparison of the ε_{Nd} record from Feni Drift to different components in ice-rafted debris extracted from sediment core MD01-2461 in the Porcupine Bight (Peck et al., 2007). (A) British Ice Sheet (BIS) debris in grains per gram of dry sediment; (B) tephra (closed symbols) and volcanics (open symbols) in grains per gram of dry sediment; and (C) the total ice rafted debris (IRD) flux of the >150 µm in cm^2/year. The grey bars represent the approximate timing of Heinrich events H1 to H4 and the Younger Dryas (YD), adopted from Hemming (2004).

Table DR1: The core depth (metres composite depth), age (calendar kyr before present), the concentration in μg Nd per gram of dried sediment, and the ε_{Nd} compositions of the Fe-Mn oxyhydroxide fraction.

Core section	Depth (mcd)	Age (cal kyr BP)	Nd (μg/g)	$^{143}Nd/^{144}Nd$	2 SE	ε_{Nd}	2 SE
162-980B-1H-1	0.3	2.1	6.51	0.512119	0.000005	-10.13	0.09
162-980B-1H-1	0.53	2.95	1.81	0.512124	0.000008	-10.02	0.16
162-980B-1H-1	0.61	3.24	1.59	0.512126	0.000009	-10.00	0.18
162-980B-1H-1	0.67	3.45	1.3	0.512117	0.000010	-10.17	0.19
162-980B-1H-1	1.05	4.87	1.87	0.512125	0.000007	-10.27	0.13
162-980B-1H-2	1.63	7.01	0.32	0.512107	0.000010	-10.35	0.20
162-980B-1H-2	1.72	7.34	2.19	0.512022	0.000005	-12.02	0.09
162-980B-1H-2	1.88	7.93	2.79	0.512009	0.000003	-12.27	0.07
162-980B-1H-2	2.03	8.48	3.79	0.512035	0.000002	-12.02	0.04
162-980B-1H-2	2.43	9.96	1.61	0.512110	0.000004	-10.58	0.08
162-980B-1H-2	2.75	11.14	0.96	0.512143	0.000005	-9.65	0.09
162-980B-1H-2	2.99	12.09	1.02	0.512122	0.000005	-10.06	0.11
162-980B-1H-3	3.16	12.91	1.08	0.512131	0.000006	-9.89	0.11
162-980B-1H-3	3.24	13.3	0.97	0.512111	0.000006	-10.29	0.12
162-980B-1H-3	3.48	14.46	1.48	0.512137	0.000004	-10.05	0.08
162-980B-1H-3	3.72	15.62	2.36	0.512248	0.000004	-7.60	0.09
162-980B-1H-3	3.88	16.39	2.04	0.512223	0.000004	-8.10	0.08
162-980B-1H-3	3.96	16.78	1.06	0.512153	0.000004	-9.46	0.09
162-980B-1H-3	4.04	17.16	0.84	0.512137	0.000004	-9.76	0.08
cc section	4.12	17.55	0.92	0.512138	0.000006	-9.75	0.11
162-980A-1H-1	4.29	18.37	0.77	0.512103	0.000005	-10.44	0.10
162-980A-1H-1	4.69	19.65	5.54	0.512160	0.000005	-9.60	0.09
162-980A-1H-1	4.85	20.19	0.96	0.512243	0.000008	-7.70	0.15
162-980A-1H-1	5.01	20.73	0.65	0.512177	0.000011	-8.99	0.22
162-980A-1H-1	5.57	22.61	0.76	0.512118	0.000004	-10.14	0.09
162-980A-1H-2	5.73	23.14	0.94	0.512169	0.000005	-9.15	0.10
162-980A-1H-2	5.97	23.84	0.88	0.512194	0.000004	-8.66	0.07
162-980A-1H-2	6.29	26.65	1.03	0.512114	0.000005	-10.22	0.09
162-980A-1H-2	6.77	30.86	0.11	0.512128	0.000010	-9.96	0.20
162-980A-1H-2	6.85	31.56	0.45	0.512233	0.000020	-8.16	0.39
162-980A-1H-2	6.93	32.26	0.83	0.512153	0.000009	-9.74	0.18
162-980A-1H-2	7.09	33.67	0.93	0.512162	0.000011	-9.56	0.21
162-980A-1H-3	7.25	35.07	1.28	0.512119	0.000005	-10.13	0.09
162-980A-1H-3	7.41	36.47	1.07	0.512155	0.000011	-9.42	0.22
162-980A-1H-3	7.49	37.17	1.1	0.512121	0.000011	-10.09	0.22
162-980A-1H-3	7.73	39.28	0.1	0.512074	0.000006	-11.00	0.11
162-980A-1H-3	7.81	39.98	0.18	0.512150	0.000007	-9.52	0.13
162-980A-1H-3	7.89	40.68	0.17	0.512136	0.000004	-9.79	0.07
162-980A-1H-3	8.05	42.09	0.16	0.512183	0.000011	-8.87	0.21

Table DR2: The core depth (metres composite depth), age (calendar kyr before present), the concentration in μg Nd per gram of dried sediment, and the ε_{Nd} compositions of the detrital fraction.

Core section	Depth (mcd)	Age (cal kyr BP)	Nd (μg/g)	$^{143}Nd/^{144}Nd$	2 SE	ε_{Nd}	2 SE
162-980A-1H-2	5.97	23.84	20	0.512021	0.000005	-12.04	0.10
162-980A-1H-2	6.29	26.65	22	0.511989	0.000004	-12.65	0.08
162-980A-1H-2	6.77	30.86	nm	0.512039	0.000005	-11.68	0.09
162-980A-1H-3	7.73	39.28	20	0.511914	0.000004	-14.12	0.07
162-980A-1H-3	7.81	39.98	20	0.511965	0.000004	-13.12	0.08
162-980A-1H-3	7.89	40.68	20	0.511989	0.000005	-12.66	0.10
162-980A-1H-3	8.05	42.09	14	0.511994	0.000004	-12.56	0.08

Table DR3: The core depth (metres composite depth), age (calendar kyr before present), the concentration in µg Sr per gram of dried sediment, and the $^{87}Sr/^{86}Sr$ isotope compositions of the Fe-Mn oxyhydroxide and detrital fractions.

Core section	Core depth (mcd)	Age (cal kyr BP)	Sr (µg/g)	$^{87}Sr/^{86}Sr$	2 SE
FeMn oxyhydroxide fraction					
162-980B-1H-1	0.30	2.1	4.45	0.709997	0.000022
162-980B-1H-1	0.53	2.9	4.57	0.709284	0.000009
162-980B-1H-1	0.61	3.2	3.75	0.709424	0.000012
162-980B-1H-1	0.67	3.4	4.19	0.709361	0.000013
162-980B-1H-1	1.05	4.9	2.41	0.709554	0.000019
162-980B-1H-2	1.63	7.0	158.08	0.709120	0.000012
162-980B-1H-2	2.03	8.5	93.88	0.709111	0.000010
162-980B-1H-2	2.43	10.0	4.95	0.709485	0.000014
162-980B-1H-2	2.75	11.1	2.55	0.710323	0.000012
162-980B-1H-3	3.48	14.5	3.72	0.709416	0.000012
162-980B-1H-3	3.72	15.6	6.57	0.708876	0.000012
162-980B-1H-3	3.80	16.0	8.97	0.709197	0.000011
162-980B-1H-3	4.04	17.2	4.90	0.709534	0.000014
cc section	4.12	17.6	3.65	0.709822	0.000013
162-980A-1H-1	4.29	18.4	3.37	0.709529	0.000011
162-980A-1H-1	4.69	19.7	14.01	0.709881	0.000013
162-980A-1H-1	4.85	20.2	0.53	0.709710	0.000018
162-980A-1H-1	5.01	20.7	0.17	0.711193	0.000047
162-980A-1H-1	5.57	22.6	2.74	0.709860	0.000011
162-980A-1H-2	5.97	23.8	3.00	0.709560	0.000012
162-980A-1H-2	6.29	26.6	2.95	0.709706	0.000011
162-980A-1H-2	6.77	30.9	2.82	0.710246	0.000011
162-980A-1H-2	6.85	31.6	0.92	0.711309	0.000038
162-980A-1H-2	7.09	33.7	1.62	0.712070	0.000033
162-980A-1H-3	7.25	35.1	3.32	0.709941	0.000008
162-980A-1H-3	7.41	36.5	1.26	0.710683	0.000020
162-980A-1H-3	7.49	37.2	1.73	0.711695	0.000031
162-980A-1H-3	7.73	39.3	2.80	0.711100	0.000016
162-980A-1H-3	7.81	40.0	2.00	0.711824	0.000014
162-980A-1H-3	7.89	40.7	2.66	0.710189	0.000010
162-980A-1H-3	8.05	42.1	2.25	0.710703	0.000021
Duplicates of the FeMn oxyhydroxide fraction					
162-980A-1H-3	7.73	39.28	3.3	0.711073	0.000010
162-980A-1H-3	7.89	40.68	2.5	0.710108	0.000008
162-980A-1H-3	8.05	42.09	3.3	0.709890	0.000012
Detrital fraction					
162-980A-1H-2	5.97	23.84	111	0.725944	0.000010
162-980A-1H-2	6.29	26.65	138	0.725390	0.000010
162-980A-1H-2	6.77	30.86	112	0.723236	0.000008
162-980A-1H-3	7.73	39.28	137	0.726398	0.000008
162-980A-1H-3	7.81	39.98	144	0.726598	0.000009
162-980A-1H-3	7.89	40.68	138	0.725589	0.000007
162-980A-1H-3	8.05	42.09	107	0.724210	0.000009

Table DR4: Modelling parameters used to calculate the effect of Lake Agassiz drainage waters on North Atlantic surface ocean ε_{Nd}.

surface area of the North Atlantic and surrounding ocean basins	5.32×10^7 km^2
depth of surface ocean layer	100 m
Nd concentration in surface ocean	3 pg/g
total Nd in North Atlantic surface ocean	1.6×10^{22} pg
ε_{Nd} of surface ocean (North Atlantic)	-14
ε_{Nd} of surface ocean (Norwegian Sea)	-13
Nd released during the drainage event	2×10^{21} pg
ε_{Nd} of drainage waters	-25

References:

Barber, D.C., Dyke, A., Hillaire-Marcel, C., Jennings, A.E., Andrews, J.T., Kerwin, M.W., Bilodeau, G., McNeely, R., Southon, J., Morehead, M.D., and Gagnon, J.M., 1999, Forcing of the cold event of 8,200 years ago by catastrophic drainage of Laurentide lakes: Nature, v. 400, p. 344-348.

Born, A., and Levermann, A., 2010, The 8.2 ka event: Abrupt transition of the subpolar gyre toward a modern North Atlantic circulation: Geochemistry Geophysics Geosystems, v. 11, p. Q06011.

Clarke, G.K.C., Leverington, D.W., Teller, J.T., and Dyke, A.S., 2004, Paleohydraulics of the last outburst flood from glacial Lake Agassiz and the 8200 BP cold event: Quaternary Science Reviews, v. 23, p. 389-407.

Goldstein, S.J., and Jacobsen, S.B., 1987, The Nd and Sr isotopic systematics of river-water dissolved material: Implications for the sources of Nd and Sr in seawater: Chemical Geology: Isotope Geoscience section, v. 66, p. 245-272.

Gutjahr, M., Frank, M., Stirling, C.H., Klemm, V., van de Flierdt, T., and Halliday, A.N., 2007, Reliable extraction of a deepwater trace metal isotope signal from Fe-Mn oxyhydroxide coatings of marine sediments: Chemical Geology, v. 242, p. 351-370.

Hagedorn, B., and Hasholt, B., 2004, Hydrology, geochemistry and Sr isotopes in solids and solutes of the meltwater from Mittivakkat Gletscher, SE Greenland: Nordic Hydrology, v. 35, p. 369-380.

Hemming, S.R., 2004, Heinrich events: Massive late pleistocene detritus layers of the North Atlantic and their global climate imprint: Reviews of Geophysics, v. 42, p. doi:10.1029/2003RG000128.

Jacobsen, S.B., and Wasserburg, G.J., 1980, Sm-Nd isotopic evolution of chondrites: Earth and Planetary Science Letters, v. 50, p. 139-155.

Jeandel, C., Arsouze, T., Lacan, F., Techine, P., and Dutay, J.C., 2007, Isotopic Nd compositions and concentrations of the lithogenic inputs into the ocean: A compilation, with an emphasis on the margins: Chemical Geology, v. 239, p. 156-164.

Lacan, F., and Jeandel, C., 2004, Neodymium isotopic composition and rare earth element concentrations in the deep and intermediate Nordic Seas: Constraints on the Iceland Scotland Overflow Water signature: Geochemistry Geophysics Geosystems, v. 5, p. doi:10.1029/2004GC000742.

Lacan, F., and Jeandel, C., 2005, Acquisition of the neodymium isotopic composition of the North Atlantic Deep Water: Geochemistry Geophysics Geosystems, v. 6, p. doi:10.1029/2005GC000956.

Martinson, D.G., Pisias, N.G., Hays, J.D., Imbrie, J., Moore, T.C., and Shackleton, N.J., 1987, Age dating and the orbital theory of the ice ages: Development of a high-resolution 0 to 300,000-year chronostratigraphy: Quaternary Research, v. 27, p. 1-29.

McManus, J.F., Oppo, D.W., and Cullen, J.L., 1999, A 0.5-Million-Year Record of Millennial-Scale Climate Variability in the North Atlantic: Science, v. 283, p. 971-975.

Mertz, D.F., and Haase, K.M., 1997, The radiogenic isotope composition of the high-latitude North Atlantic mantle: Geology, v. 25, p. 411-414.

Peck, V.L., Hall, I.R., Zahn, R., Grousset, F., Hemming, S.R., and Scourse, J.D., 2007, The relationship of Heinrich events and their European precursors over the past 60 ka BP: a multi-proxy ice-rafted debris provenance study in the North East Atlantic: Quaternary Science Reviews, v. 26, p. 862-875.

Rutberg, R.L., Hemming, S.R., and Goldstein, S.L., 2000, Reduced North Atlantic deep water flux to the glacial Southern Ocean inferred from neodymium isotope ratios: Nature, v. 405, p. 935-938.

Shackleton, N.J., Berger, A., and Peltier, W.R., 1990, An Alternative Astronomical Calibration of the Lower Pleistocene Timescale Based on ODP Site 677: Transactions of the Royal Society of Edinburgh-Earth Sciences, v. 81, p. 251-261.

Sherwin, T.J., Griffiths, C.R., Inall, M.E., and Turrell, W.R., 2008, Quantifying the overflow across the Wyville Thomson Ridge into the Rockall trough: Deep-Sea Research Part I-Oceanographic Research Papers, v. 55, p. 396-404.

Sherwin, T.J., and Turrell, W.R., 2005, Mixing and advection of a cold water cascade over the Wyville Thomson Ridge: Deep-Sea Research Part I-Oceanographic Research Papers, v. 52, p. 1392-1413.

Teller, J.T., Leverington, D.W., and Mann, J.D., 2002, Freshwater outbursts to the oceans from glacial Lake Agassiz and their role in climate change during the last deglaciation: Quaternary Science Reviews, v. 21, p. 879-887.

Vance, D., Scrivner, A.E., Beney, P., Staubwasser, M., Henderson, G.M., and Slowey, N.C., 2004, The use of foraminifera as a record of the past neodymium isotope composition of seawater: Paleoceanography, v. 19.

Vance, D., and Thirlwall, M., 2002, An assessment of mass discrimination in MC-ICPMS using Nd isotopes: Chemical Geology, v. 185, p. 227-240.

von Grafenstein, U., Erlenkeuser, H., Muller, J., Jouzel, J., and Johnsen, S., 1998, The cold event 8200 years ago documented in oxygen isotope records of precipitation in Europe and Greenland: Climate Dynamics, v. 14, p. 73-81.